

2023

Interactions of Carboxylated Nanodiamonds With Mouse Macrophages Cell Line and Primary Cells

Maisoun Bani-Hani
Old Dominion University, mbanihan@odu.edu

Stephen J. Beebe
Old Dominion University, sbeebe@odu.edu

Michael W. Stacey
Old Dominion University, mstacey@odu.edu

Christopher Osgood
Old Dominion University, cosgood@odu.edu

Follow this and additional works at: https://digitalcommons.odu.edu/bioelectrics_pubs



Part of the [Biomedical Engineering and Bioengineering Commons](#), [Cells Commons](#), and the [Nanomedicine Commons](#)

Original Publication Citation

Bani-Hani, M., Beebe, S. J., Stacey, M. W., & Osgood, C. (2023). Interactions of carboxylated nanodiamonds with mouse macrophages cell line and primary cells. *International Journal of Orthopaedics Research*, 6(1), 30-43. <https://www.opastpublishers.com/peer-review/interactions-of-carboxylated-nanodiamonds-with-mouse-macrophages-cell-line-and-primary-cells-5344.html>

This Article is brought to you for free and open access by the Frank Reidy Research Center for Bioelectrics at ODU Digital Commons. It has been accepted for inclusion in Bioelectrics Publications by an authorized administrator of ODU Digital Commons. For more information, please contact digitalcommons@odu.edu.

Interactions of Carboxylated Nanodiamonds With Mouse Macrophages Cell Line and Primary Cells

Maisoun Bani-Hani^{1,2}, Stephen J Beebe¹, Michael W Stacey¹ and Christopher Osgood^{2*}

¹Frank Reidy Research Center for Bioelectrics, Old Dominion University, Norfolk, Virginia, USA

²Department of Biological Sciences, Old Dominion University, Norfolk, Virginia, USA

*Corresponding author

Christopher Osgood, Department of Biological Sciences, Old Dominion University, Norfolk, Virginia, USA

Submitted: 28 Feb 2023; Accepted: 23 Mar 2023; Published: 31 Mar 2023

Citation: Bani-Hani, M., Beebe, S. J., Stacey, M. W., Osgood, C. (2023). Interactions of Carboxylated Nanodiamonds With Mouse Macrophages Cell Line and Primary Cells. *Int J Ortho Res*, 6(1), 30-43.

Abstract

Nanodiamonds (ND) have attracted significant interest for their use in several biomedical applications. These applications can be very useful if the safety and compatibility of ND are proven. We assessed the effects of ND (100 nm, Carboxylated) on primary macrophages and a macrophage-like cell line and found that these particles are not toxic to these cells at lower concentrations but may interfere with cell functions and differentiation. Internalization of ND by these cells in a time- and dose-dependent manner was mostly via phagocytosis and clathrin-dependent endocytosis and localized to the cytoplasm but not into the nucleus. No significant induction of inflammatory cytokines or reduction in the ability of these cells to respond to lipopolysaccharides (LPS) was noted. However, the endocytic activity of these cells is significantly reduced. In addition, ND exposure reduced the ability of differentiating bone marrow cells to express macrophage surface markers. Measurement of the fluorescence and absorbance of ND-treated cells clearly showed the ability of these particles to produce a signal at different wavelengths. Therefore, it is important to consider interference of ND in different colorimetric and fluorometric assays when testing interactions or effects of ND on cells. Our findings suggest that ND are not cytotoxic to macrophages at the tested concentrations, but it can interfere with macrophage functions and differentiation and may interfere with assays' result through the production of a signal at different wavelengths.

Keywords: Nanodiamonds, macrophages, immunotoxicity, inflammatory response, differentiation, endocytic activity.

Introduction

The field of nanomedicine has attracted much interest because of its high potential for improving diagnosis and treatment modalities. The ability to manipulate nanosized particles with enhanced physical, chemical, and biological characteristics has led to many different biomedical applications using a wide variety of nanoparticles [1, 2]. Carbon-based nanomaterials with different sizes, shapes, and surface chemistries, such as single- and multi-walled carbon nanotubes, fullerenes, graphene, and nanodiamonds (ND), have been extensively investigated for biomedical applications [3-6]. Among these materials, ND is the most biocompatible carbon-based nanomaterial [7-14]. Therefore, ND has been investigated for use in different biomedical applications including coating of orthopedic implants which shows enhanced biocompatibility and bioactivity [15]. However, some reports have shown the toxic effects of ND both in vitro and in vivo [16-19].

Introducing foreign materials, such as nanoparticles, into the body may lead to their recognition by immune cells, initiation of an immune response, modulation, or even depletion of immune cell function (20). Any negative effect on immune cell viability, proliferation, differentiation, or function is considered immu-

notoxicity, which can be induced by exposure to nanoparticles, leading to detrimental effects on the immune system and the whole body [21]. Nonspecific innate immune cells usually recognize and initiate a response to any foreign substance or organism and have been used extensively in immunotoxicity studies of nanoparticles. Activation of immune cells by many different types of nanoparticles has been reported in several studies [22-25]. In addition, the suppression of immune cell functions after exposure to nanoparticles, such as carbon nanotubes, has also been reported [26-29].

The effects of ND on immune cells may include suppression or over-stimulation and thus need to be further evaluated. We aimed to study the interactions of ND with macrophages and showed that these particles are non-cytotoxic at lower concentrations but can interfere with the ability of macrophages to endocytose other materials and differentiate them from primary mouse bone marrow cells.

Materials and methods

Nanodiamonds and cell culture

Carboxylated, High pressure-high temperature ND with an average size of 100 nm, containing >900 nitrogen vacancies (NV,

which are point defects in the diamond lattice responsible for producing the fluorescence of the ND) /particle and excitation/emission of 532/700 nm (Adamas Nanotechnologies, Inc. Raleigh, NC) were sonicated for 10-15 minutes in a water bath sonicator before each use and suspended in cell culture media at concentrations of 1-100 µg/ml.

The J774A.1 cell line (American Type Culture Collection, Manassas, VA) and mouse bone marrow-derived macrophages (BMDM). The J774A.1 cells were maintained in Dulbecco's modified Eagle's medium (DMEM, Lonza, USA) supplemented with 10% heat-inactivated fetal bovine serum (FBS, Gibco, USA), 100 units/ml penicillin, and 100 µg/ml streptomycin (Gibco) at 37°C in a 5% CO₂ humidified incubator. Primary cells were isolated and differentiated directly or frozen, as previously described, with some modifications [30,31]. Briefly, C57BL/6, CD-1, DBA/2J, and BALB/cJ, mice 1-4 months old, were euthanized in a CO₂ chamber. Femurs and tibias were flushed with phosphate buffer saline (PBS), passed through a 40 µm cell strainer (Celltreat), centrifuged at 200 g for 5 min, and resuspended in freezing media (90% FBS and 10% DMSO) or plated directly in differentiation media: RPMI 1640 (Mediatech Manassas, VA) supplemented with 20% FBS, 100 units/ml penicillin, 100 µg/ml streptomycin, and 10 ng/ml macrophage-colony stimulating factor (M-CSF, Biolegend, San Diego, CA) at 37°C in a 5% CO₂ humidified incubator. After seven days, cells were harvested by scraping or detachment with 5 mM EDTA/PBS, counted, and plated with cultivation media (same constituent as differentiation media, except FBS was decreased to 10%). Mouse femurs and tibias were obtained through tissue sharing from IACUC-approved protocols (14-003, 14-007, 15-027, 16-016). Macrophages were identified as double positive for CD11b and F4/80 surface markers. Cells were suspended in flow buffer (1% bovine serum albumin [BSA] in PBS) with a blocking antibody (CD 16/32) for 10 min. One microliter of FITC-CD11b and PE-F4/80 (AbD Serotec®) was added and incubated in the dark at room temperature. After 30 min, the cells were washed and re-suspended in 300 µL flow buffer for fluorescence-activated cell sorting (FACS) analysis (BD FACSAria™ cell sorter BD Biosciences San Jose, CA).

Cell Viability Assays

MTS viability assay (CellTiter 96® Aqueous Non-Radioactive

Cell Proliferation Assay, Promega) was used to assess cell viability. Cells were plated at 2-3 x 10⁴ cells per well in a 96-well plate for 24 h, and then ND was applied at the indicated concentrations and time intervals for each experiment. After treatment, the medium was replaced and MTS reagent was added directly or 1, 2, or 3 days after ND treatment. After 2-4 hours, the supernatants were transferred into new wells and the absorbance was measured at 490 nm using a plate reader (SpectraMax i3, Molecular Devices). Cell viability was determined by normalizing the absorbance of the ND-treated cells to that of the control and untreated cells and expressed as a percentage.

Cell death was measured using the apoptosis assay kit according to the manufacturer's instructions, except for the last step of adding the red dead cell stain (SYTOX™ AADvanced™), which differentiates apoptotic cells from necrotic cells, which was not used because of ND interference with the red fluorescent stain (CellEvent™ Caspase- 3/7 Green Flow Cytometry Assay Kit, Thermo Fisher). Cells were plated at 10⁵ cells/well in 6-well plates for 24 h before incubation with 10, 50, or 100 µg/ml ND for another 24 h, with untreated cells as a negative control, and 10 µM staurosporine (Sigma) or 100 ng/ml lipopolysaccharides (LPS) (Sigma) as positive controls.

ND Uptake And Subcellular Localization

Microscopic slides were prepared by plating cells on coverslips for 24 h, followed by treatment with 50 µg/ml ND for another 24 h, staining with DAPI, and viewing with fluorescent microscopy (Olympus BX51) and confocal microscopy to determine their subcellular localization (Leica TCS SP8, Leica Microsystems).

To quantify ND uptake, cells were plated at 10⁵ cells/well in 6-well plates for 24 h and treated with the indicated ND concentrations and time intervals. Each sample was harvested, centrifuged for 5 min at 200 × g, and resuspended in flow buffer before FACS analysis.

Endocytic pathway inhibitors (Sigma-Aldrich) were prepared and used as previously described (References in Table 1). Each inhibitor was incubated with cells for 30 min at 37°C prior to ND treatment. The uptake of ND by cells pre-treated or untreated with each inhibitor was measured using FACS.

Table 1: Endocytic pathway inhibitors.

Inhibitor	Pathway	Reference	Concentration
Chlorpromazine hydrochloride	Clathrin-dependent endocytosis	32,33	20 µg/ml
Phenylarsine oxide	Clathrin and receptor-mediated endocytosis	34,35	0.5 µg/ml
Methyl-beta-cyclodextrin	Caveolae and clathrin-dependent endocytosis	36,37	10 mM
Nystatin	Caveolae/lipid raft dependent endocytosis	33,38	40 µg/ml
5-(N-Ethyl-N-isopropyl) amiloride; EIPA	Macropinocytosis	39,40	66 µM
Cytochalasin D	Actin-dependent endocytosis	41	6 µM

Gene Expression

Cytokine expression was measured at both mRNA and protein levels. For RT-qPCR experiments, cells were plated at $1-2 \times 10^5$ cells/well in 12-well plates and exposed to 50 $\mu\text{g/ml}$ ND for 4 h before RNA isolation (ISOLATE II RNA Mini Kit, Bionline USA). Complementary DNA (cDNA) was synthesized using the SensiFAST™ cDNA synthesis kit (Bionline USA), and the quality and quantity of RNA and cDNA were assessed using a NanoVue (GE Healthcare). The cDNA was amplified using the SensiFAST SYBR Hi-ROX kit (Bionline USA) in a Bio-Rad

CFX Connect Real-Time PCR Detection System (Bio-Rad, USA). Primer (IDT®) sequences were obtained from previously published studies (references and sequences are summarized in Table 2). Gene expression data were normalized to that of two housekeeping genes; Glyceraldehyde-3-phosphate dehydrogenase (GAPDH) and β -actin, and the fold change was determined using the $\Delta\Delta\text{CT}$ method. To assess the ability of ND-treated cells to respond to LPS, cells were plated as described above with or without ND (50 $\mu\text{g/ml}$) for 4 h, with or without 10 ng/ml LPS (Sigma) for 3 h before RNA isolation and RT-qPCR analysis.

Table 2: RT-qPCR primers.

Gene	Forward primer	Reverse primer	Reference
GAPDH	TAT GTC GTG GAG TCT ACT GGT	GAG TTG TCA TAT TTC TCG T	42
β -Actin	TGG AAT CCT GTG GCA TCC ATG AAA C	TAA AAC GCA GCT CAG TAA CAG TCC G	42
IL1- β	CAA CCA ACA AGT GAT ATT CTC CAT G	GAT CCA CAC TCT CCA GCT GCA	43
IL 6	GAG GAT ACC ACT CCC AAC AGA CC	AAG TGC ATC ATC GTT GTT CAT ACA	43
TNF α	CCT GTA GCC CAC GTC GTA GC	AGC AAT GAC TCC AAA GTA GAC C	42
CCL2	CCC ACT CAC CTG CTG CTA CT	TCT GGA CCC ATT CCT TCT TG	44
CXCL2	CCA CTC TCA AGG GCG GTC AAA	TAC GAT CCA GGC TTC CCG GGT	17
iNOS	TTT GCT TCC ATG CTA ATG CGA AAG	GCT CTG TTG AGG TCT AAA GGC TCC G	42
IL4	AAC GAG GTC ACA GGA GAA GG	TCT GCA GCT CCA TGA GAA CA	45
IL10	ATA ACT GCA CCC ACT TCC CA	GGG CAT CAC TTC TAC CAG GT	45
IL12	GAT GAC ATG GTG AAG ACG GC	AGG CAC AGG GTC ATC ATC AA	45

The secretion of pro-inflammatory cytokines was measured using an ELISA kit (LEGENDplex™ mouse inflammation panel, Biolegend®, San Diego, CA). Cells were plated at 10^6 cell/ml in 6-well plates for 24 h, and then the medium was replaced with 50 $\mu\text{g/ml}$ ND or 10 ng/ml LPS and incubated for another 24 h. Cell culture supernatant was collected, centrifuged at 1500 RPM for 10 min at 4 °C, and stored at -80 until analysis by ELISAs.

Effects of ND on Macrophages Endocytic Activity

Bone marrow cells were plated at 10^5 cells/well in a 6-well plate for 24 h and then treated with 0, 10, 20, or 50 $\mu\text{g/ml}$ of ND. After 16 h, cells were incubated with cascade blue-labeled dextran particles (3000 MW Invitrogen, Eugene OR) for 45 min, washed, and resuspended in flow buffer for FACS analysis.

Differentiation of BMDM

Bone marrow cells were isolated as described above and differentiated into BMDM in differentiation medium with or without 50 $\mu\text{g/ml}$ ND for 7 days. Fresh media was added every 2 days, and after 7 days, cells were viewed under a microscope and labeled with macrophage surface markers (CD11b and F4/80) for FACS analysis.

Statistical Analysis

The results are presented as the mean \pm standard error of the mean (SEM) of at least three independent experiments. The test for significance was performed using one-way ANOVA for multiple comparisons, followed by Dunnett's test. Statistical sig-

nificance was set at $P < 0.05$. Statistical calculations were performed using the IBM SPSS version 24. Statistical significance was assessed using the Student's T test when comparing one treatment with one control.

Results

Interactions of ND with macrophages

The macrophage cell line (J774A.1) and primary BMDM were exposed to different concentrations of ND (0–100 $\mu\text{g/ml}$ ND) for different time points (0–24 hours), and the ND-treated or untreated cells were visualized with fluorescent and confocal microscopes and analyzed with FACS. The results showed that these cells internalized the ND spontaneously, as seen in the microscopic images (Figure 1a and b). ND appeared as dark aggregates in the bright-field images with red fluorescence in the TRITC channel. ND was localized to the cytoplasm, but not to the nucleus, as seen in the confocal microscopy images (Figure 1c). These images also show that the cell shape did not change dramatically owing to ND treatment. FACS analysis of the forward scatter ("FCS, which indicates cell size") and side scatter (SSC, which indicates cell granularity) showed that the ND-treated cell size (Figure 1d and e) decreased, while the granularity increased (Figure 1f and g) in a time- and dose-dependent manner. Figure 1(h) shows representative graphs of FACS analysis and changes in FSC and SSC of ND-treated cells (one-way ANOVA p value for FSC concentrations 0.297, FSC times 0.0649, SSC concentrations < 0.000 , SSC times 0.044).

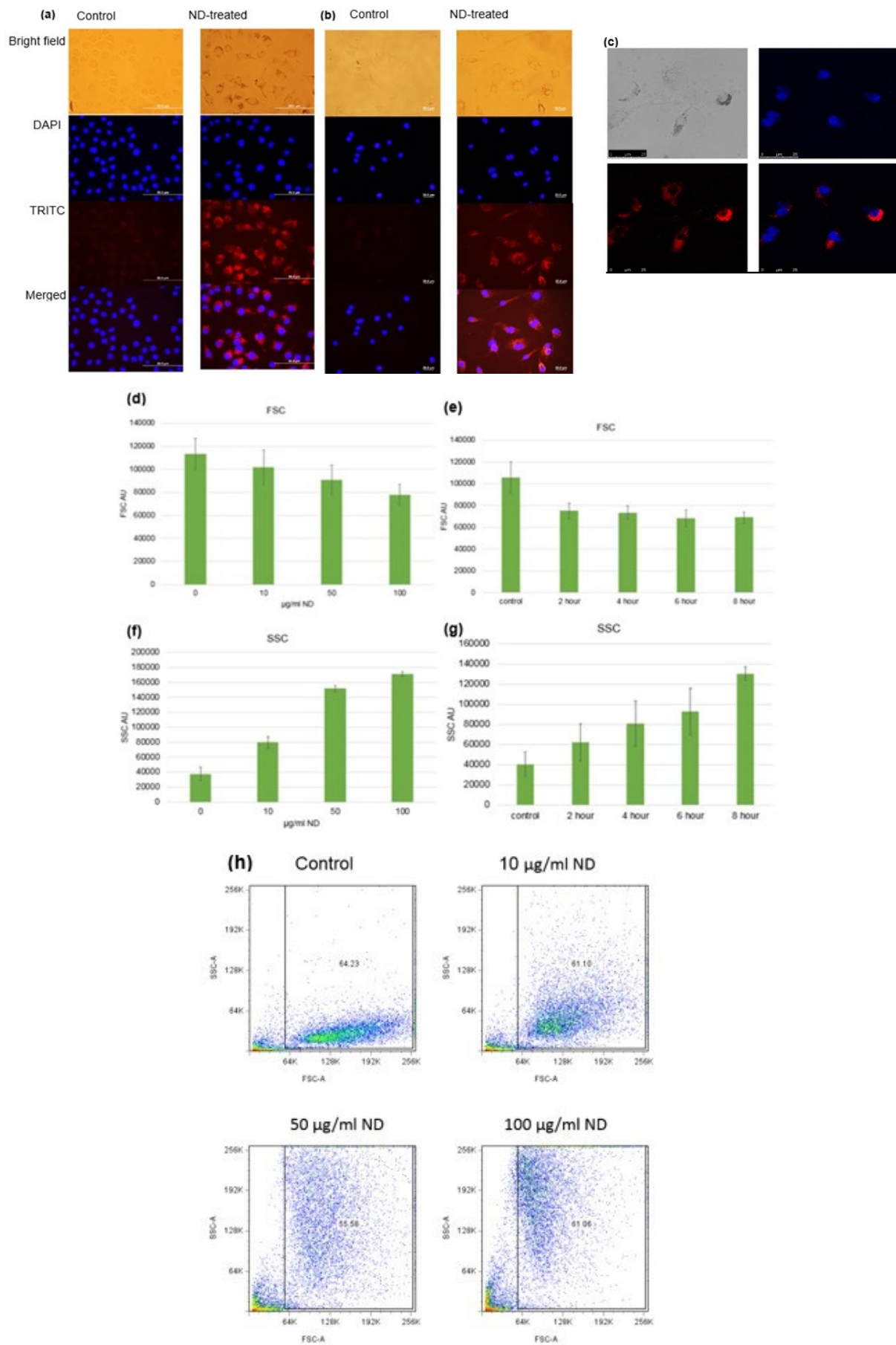


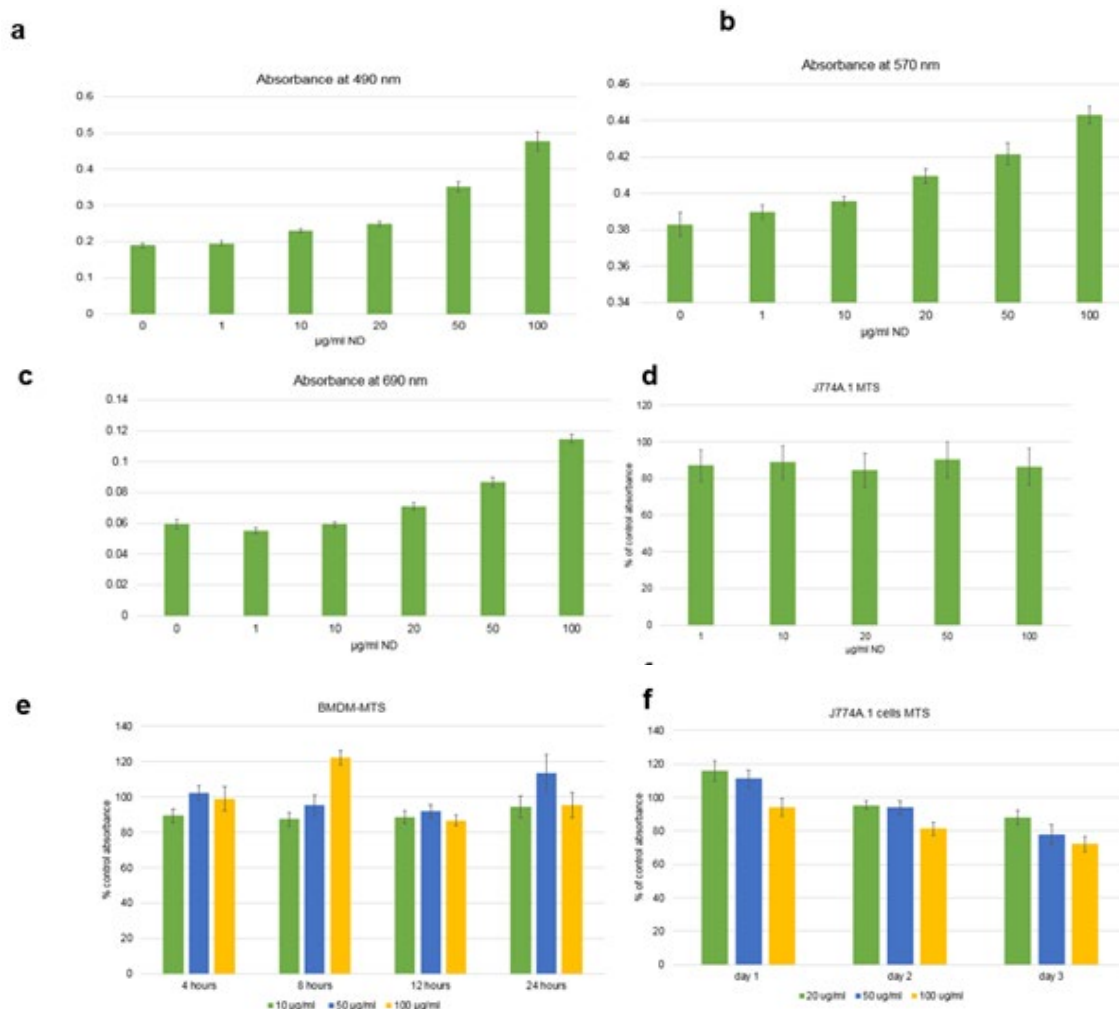
Figure 1: Internalization of ND and effects on cells' morphology.

Fluorescent microscope images of J774A.1 (a) and BMDM (b) control and ND-treated (50 $\mu\text{g/ml}$ ND for 24 hours) images from top to bottom are bright field, DAPI, TRITC, and merged images. (c) Confocal microscope images of BMDM treated with ND. DAPI staining was used to stain the nucleus. Image of bright field (top left), DAPI (top right), TRITC (bottom left), and merged (bottom right). FACS analysis of BMDM treated with 0, 10, 50, or 100 $\mu\text{g/ml}$ ND for 24 hours (d and f) or with 50 $\mu\text{g/ml}$ ND for 0, 2, 4, 6, or 8 hours (e and g). (h) Representative graphs of FACS analysis for cells treated with different concentrations of ND showed the increase in SSC (cell granularity) and decrease in FSC (cell size) with increasing ND concentration. Results represent the average of at least 3 independent experiments \pm SEM.

Cell Viability

The MTT assay was first used to determine the effects of ND on cell metabolic activity, that is, cell viability, which proved to be incompatible with the presence of ND. After exposure of the macrophage cell line to different concentrations of ND, we measured the absorbance of ND-treated and untreated cells and found that ND interfered with the absorbance measurement at all required wavelengths (Figure 2a-c). The MTT assay requires cell lysis to release the produced formazan; therefore, we decided to use the MTS assay, which does not require cell lysis to release the col-

ored formazan. After ND treatment, soluble formazan was transferred to new wells to eliminate ND interference. Cells treated with different concentrations (10-100 $\mu\text{g/ml}$ of ND for different time intervals (4-24 hours) did not show a significant reduction in metabolic activity, except for two treatments: the 100 $\mu\text{g/ml}$ ND treatment for 8 h (T-test p-value 0.003) and 10 $\mu\text{g/ml}$ ND for 12 h (T-test p-value 0.026), which showed higher (122.08%) or lower (88.68%) activities (Figure 2 d and e). To determine the effects of ND on these cells after a longer exposure time, cells were treated with 20-100 μg ND for 24 h and the MTS assay was performed at 1, 2, and 3 days after treatment (Figure 2f). The results showed changes in cell metabolic activity (72.1 - 115.85%) but were not statistically significant ($p > 0.05$). We confirmed the cell viability results using the apoptosis assay kit, which differentiates live cells from apoptotic or necrotic cells. In this kit, apoptotic cells are differentiated from live cells using the caspase 3/7 green, fluorescent dye, and necrotic cells are labeled with the red dead stain (SYTOXTM AADvancedTM). We eliminated the red dead cell stain due to the interference of ND fluorescence with this stain (Figure 2g-i). Therefore, this kit was only useful for differentiating live from dead cells (regardless of whether they were apoptotic or necrotic). The percentage of dead cells ranged from 1.34 to 1.58-fold change in cell death as compared to the control and untreated cells, with no significant difference ($p > 0.05$) at all ND concentrations used (Figure 2j).



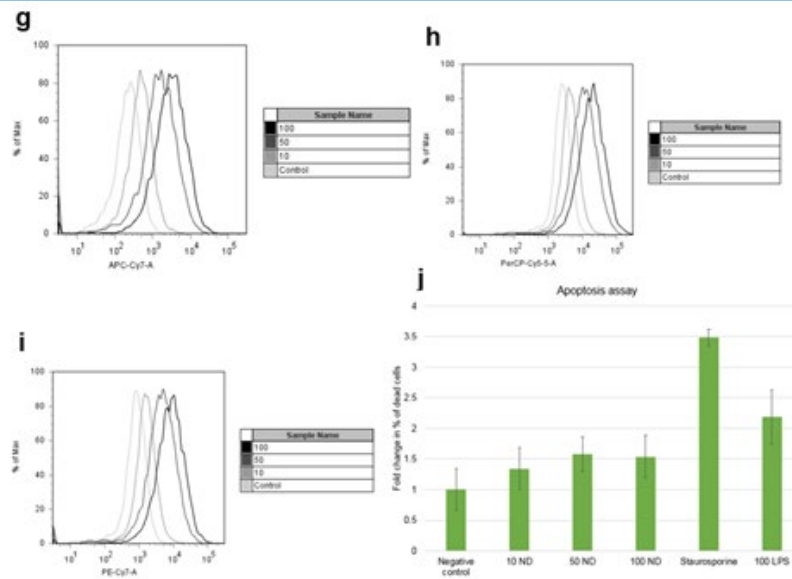


Figure 2: Viability Assays.

J774A.1 cell were treated with 0, 1, 10, 20, 50, or 100 $\mu\text{g/ml}$ ND and the absorbance was measured at 490 (a), 570 (b), and 690 (c) nm. Cell viability assay of ND-treated J774A.1 cell for 24 hours (d). (e) BMDM treated with different doses and time points, 2 days after ND treatment. One-way ANOVA was not significant except for the 100 $\mu\text{g/ml}$ ND treatment for 8 hours and 10 $\mu\text{g/ml}$ ND for 12 hours. (f) Cell viability of J774A.1 at 1, 2 and 3 days after a 24-hour ND treatment with different concentrations. One-way ANOVA from three independent experiment, each with four replicates, was not significant. BMDM were treated with different concentrations of ND (0, 10, 50, or 100 $\mu\text{g/ml}$ ND), and the fluorescence signal was measured using FACS. Results showed that fluorescence of ND can be detected in different channels including APC-Cy7 (g), PE-Cy7 (h), and PerCP-Cy5.5 (i). (j) Apoptosis assay. BMDM were treated with 10, 50, or 100 $\mu\text{g/ml}$ ND for 24 hours. Negative control is untreated cells and positive controls are 100 ng/ml LPS and 20 μM staurosporine for 24 hours. Results are average \pm SEM from at least three independent

experiments.

Quantitation of ND Uptake And Their Internalization Mechanism

The fluorescence of ND was clearly detected on multiple channels using FACS (Figure 2g-i) and the results showed an increased intensity with increasing ND concentrations and incubation times (Figure 3a and b). Multiple endocytic pathway inhibitors were used prior to ND treatment to determine the uptake mechanisms. We found that ND uptake was mostly mediated by actin- and clathrin-dependent pathways (Figure 3c). The uptake was reduced by approximately 40% when cells were pretreated with cytochalasin D, an inhibitor of actin-dependent pathways. In addition, the clathrin-dependent pathway inhibitor chlorpromazine hydrochloride reduced the uptake by approximately 20%. This is similar to previous studies showing multiple pathways used by cells for uptake.

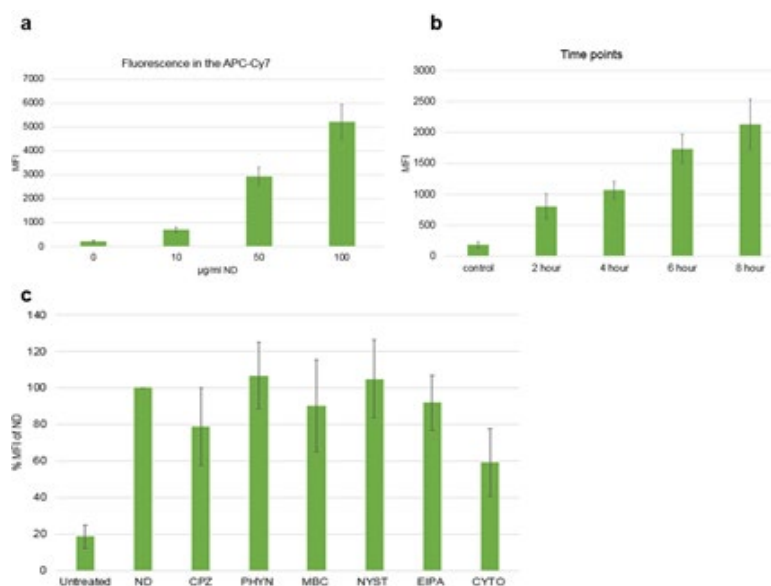


Figure 3: ND uptake.

FACS analysis of BMDM treated with 0, 10, 50, or 100 $\mu\text{g/ml}$ ND for 24 hours (a) or with 50 $\mu\text{g/ml}$ ND for 0, 2, 4, 6, and 8 hours (b). Results represent average of the Mean fluorescence intensity (MFI) of cells in arbitrary unit \pm SEM from three independent experiments. (c) FACS results showing the uptake of ND by cells pre-treated or untreated with endocytic pathways inhibitor. BMDM were pretreated with each inhibitor for 30 minutes before exposing them to ND. Abbreviations, CPZ: chlorpromazine hydrochloride, PHYN: phenylarsine oxide, MBC: methyl-beta-cyclodextrin, NYST: nystatin, EIPA: 5-(N-Ethyl-N-isopropyl) amiloride, CYTO: cytochalasin D.

Effects of ND on Gene Expression In Macrophages

Changes in gene expression in response to ND were assessed by RT-qPCR and ELISA. The expression of inflammatory cytokines IL1 β , IL6, TNF α , and iNOS, and chemokines CXCL2 and CCL2 was determined in both cell types using RT-qPCR. In addition to these genes, BMDM were assessed for IL4, IL10, and IL12

expression after ND treatment. The responses of the two cell types to ND treatment showed some variation, although none of these were statistically significant ($P > 0.05$) (Figure 4a and b). Upregulation of iNOS expression was detected in BMDM but not in J774A.1. In addition, the J774A.1 cell line showed some upregulation (2.35-, 1.56-, 2.78-, and 2.62-fold changes in the expression of IL1 β , TNF α , CXCL2, and CCL2, respectively) in the pro-inflammatory genes, except for IL6 (-1.09-fold change), whereas BMDM showed downregulation in most genes (-1.52-, -2.23-, -1.16-, -1.36, and -1.24 fold change in the expression of IL1 β , IL6, IL4, IL10, and IL12, respectively), except for TNF α (-1.04 fold change), CXCL2 (1.00 fold change), and CCL2 (1.24 fold change), which were unaffected. The expression levels were also measured in BMDM using ELISA assays for IL1 β , IL6, TNF α , IL10, and IL12; these did not change in response to ND treatment, whereas a significant increase was detected in the expression of CCL2 (Figure 4c-g).

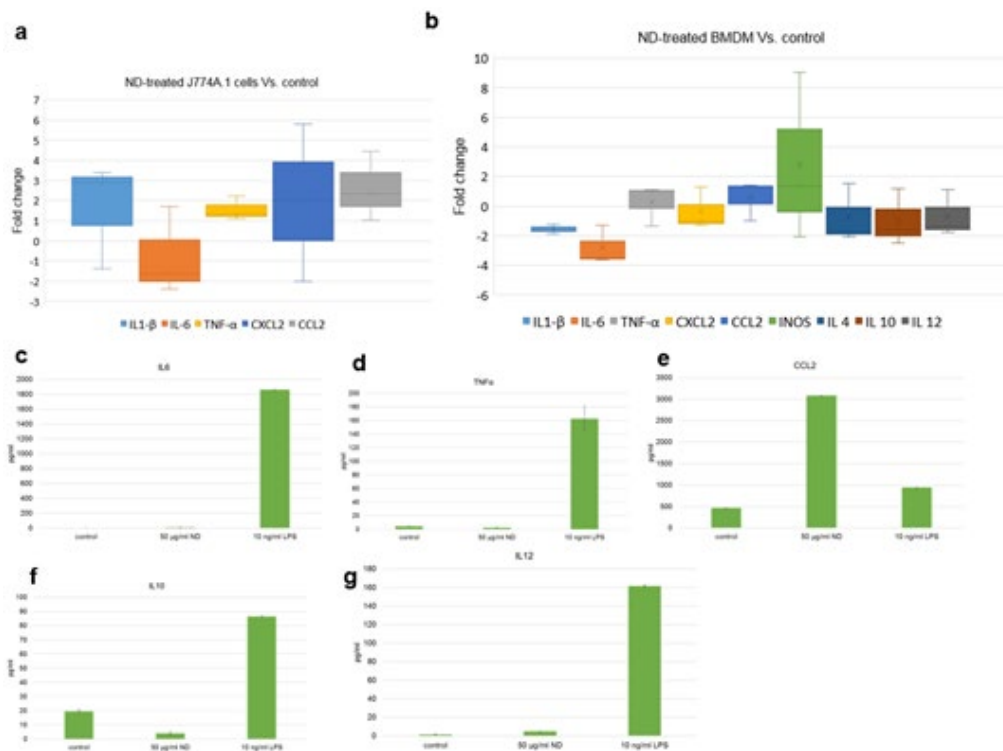


Figure 4: Gene expression in macrophages in response to ND.

Macrophage cell line, J774A.1 (a), and BMDM (b) exposed to 50 $\mu\text{g/ml}$ ND for 6-7 hours and the total RNA was isolated, converted to cDNA, and used for the RT-qPCR. Results obtained using the $\Delta\Delta\text{Ct}$ method and represent the mean fold change averaged from three independent experiment \pm SEM. Student's T test was not significant for all the tested genes ($P > 0.05$). (c-g) Cytokines ELISAs. BMDM were treated with or without 50 $\mu\text{g/ml}$ ND or 10 ng/ml LPS. After 24 hours, media were replaced, and cells were incubated for another 24 hours before collecting the supernatant for ELISAs. Results showed no effect of ND treatment on the expression of the tested cytokines except for CCL2. Results are average of two replicates \pm coefficient of variation (CV).

Effects of ND on Macrophages Functions And Differentiation

To determine the effects of ND treatment on macrophage function, the cells were treated with ND before exposure to LPS. Pretreatment of these cells with ND did not affect their ability to respond to LPS (Figure 5a and b). Changes in gene expression were not significant between the two cell types; however, slight differences were detected in their responses. The macrophage cell line showed more variability than BMDM in the expression of IL1 β (-1.00+2.67-fold change), a slight increase in IL6 (1.67-fold change) and CXCL2 (1.38-fold change), and downregulation of CCL2 (-1.49-fold change), whereas primary BMDM expression was unaffected by ND treatment.

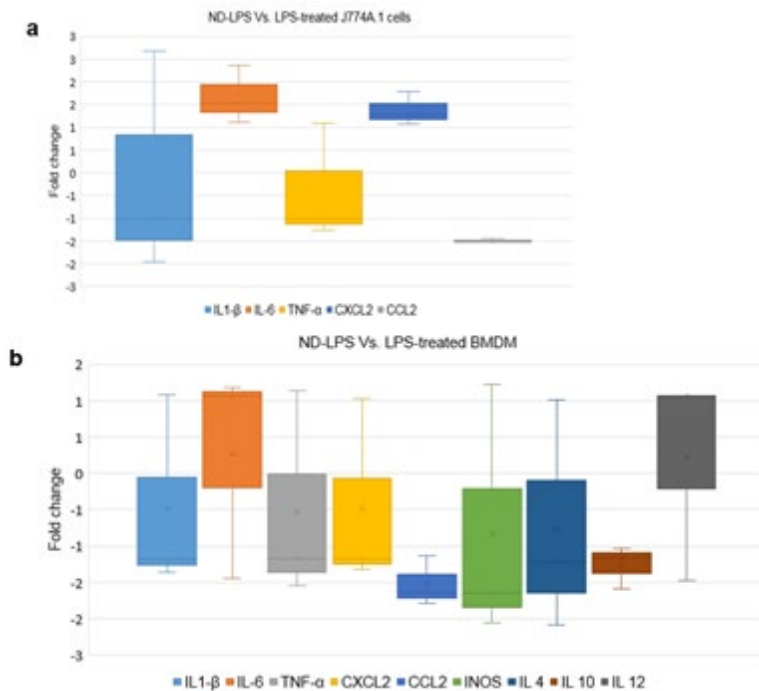


Figure 5: Effects of ND treatment on macrophages response to LPS.

RT-qPCR results showing gene expression of cytokines in J774A.1 cells (a) and BMDM (b). Cells were pretreated with 50 µg/ml ND for 4 hours before exposing them to LPS for 3 hours. The results represent the mean fold change ±SEM.

The endocytic activity of macrophages, an important function of macrophages, has also been studied. Cells were pre-treated with different concentrations of ND before being exposed to

fluorescently labeled dextran particles (3000 MW). The results showed that the ability of these cells to endocytose dextran was significantly reduced (one-way ANOVA sig 0.047, Dunnett t test (2-sided sig 0.048, 0.069, and 0.038 compared to the control with 10, 20, and 50 µg/ml ND, respectively) at all ND concentrations (64.04, 67.95, and 61.28 mean fluorescence intensity fold change for cells treated with 10, 20, and 50 µg/ml, respectively) (Figure 6).

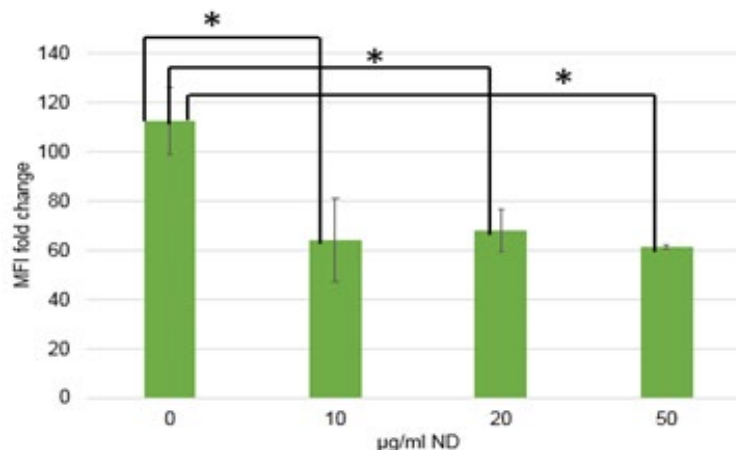


Figure 6: Endocytic activity. ND-treated and untreated BMDM were exposed to ND for 16 hours before exposing them to dextran for 45 minutes and the fluorescence signal from cells was measured using FACS. MFI results represent the mean ±SEM from three independent experiments. One-way ANOVA and Dunnett t for multiple comparisons were significant ($p < 0.05$).

Expression of Macrophage Surface Markers

As described in the Methods section, cells were prepared from mouse bone marrow in vitro for seven days with M-CSF to produce BMDM. Cells were incubated with ND from the first day after isolation from the bone marrow to study the effects of ND on differentiating cells. After 7 days, ND-treated and untreated cells were viewed under a microscope and analyzed for their ability to express the macrophage surface markers CD11b and

F4/80 using FACS (Figure 7). Cell morphology did not appear to be affected by the ND treatment (Figure 7a). The percentage of cells expressing these two surface markers was not affected (Figure 7b-d). However, the fluorescence intensities, which indicate the number of surface markers expressed on these cells, were reduced significantly with $p > 0.042$ for CD11b and $p > 0.008$ for F4/80 (Figure 7e).

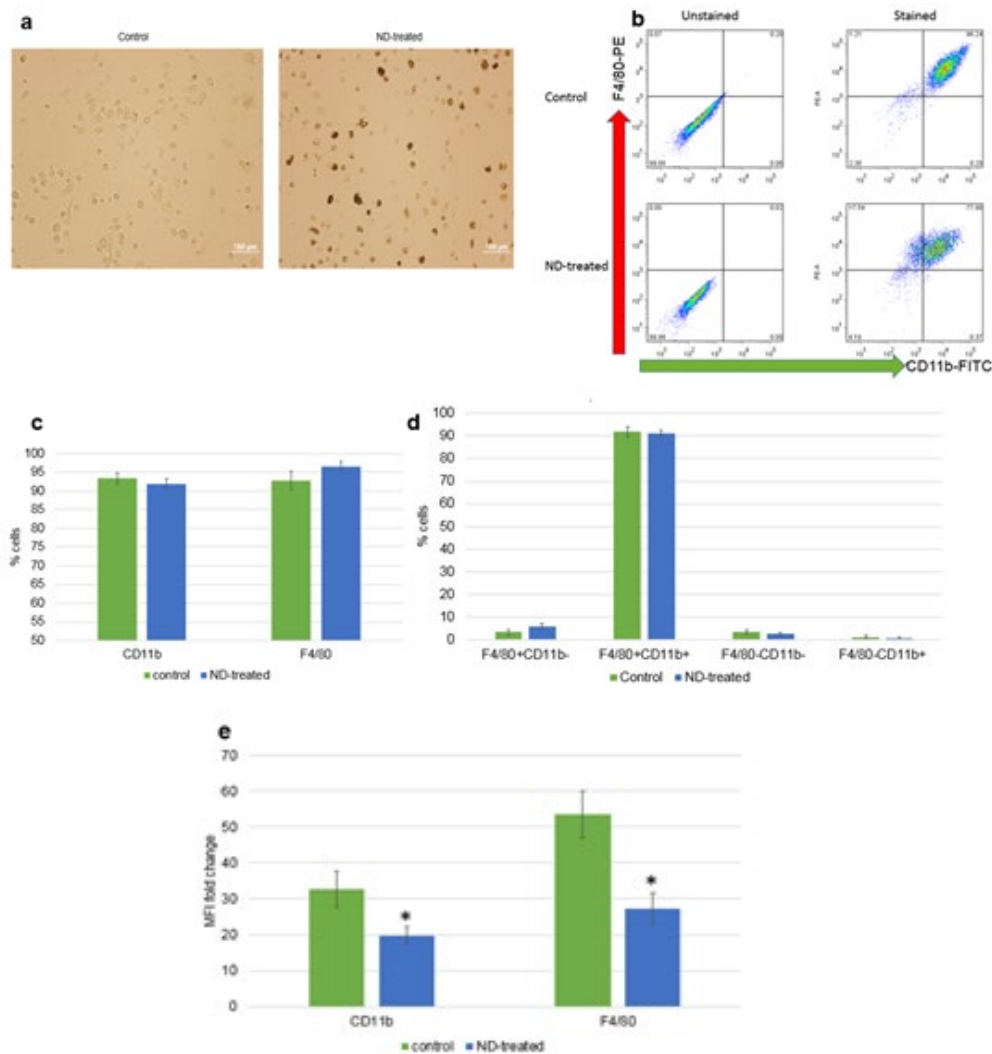


Figure 7: Effects of ND on macrophages differentiation. (a) Microscopic images of BMDM differentiated in the presence of ND. Isolated bone marrow cells were exposed to 50 $\mu\text{g/ml}$ ND and incubate for 7 days with differentiation media. Bright field images showing ND-treated (right) and untreated (left) cells. (b) Representative graphs from FACS analysis showing the percent of cells expressing macrophage surface markers, FITC-CD11b and PE-F4/80. (c) Percent of cells expressing CD11b or F4/80. (d) Percent of each cell population based on their surface markers. (e) Effects of ND on the number of surface markers expressed per cell. Results represent fold change in MFI as compared to unstained control from four independent experiments. * $p < 0.05$.

Discussion

The field of nanomedicine has attracted attention in recent years, owing to its advantages in various biomedical applications. In addition, the need to investigate the interactions and effects of nanomaterials on biological systems has been increasing. Several carbon-based nanoparticles have been the focus of research, and among these, ND stands out as the most biocompatible material [7-11]. We aimed to assess the effects of ND on macrophages using the macrophage cell line, J774A.1 and primary BMDM.

Our results showed some variation in the effects of ND between the two cell types. Cell lines have been used extensively in cytotoxicity studies. However, continuous culturing of cells in vitro results in the loss of genes that might not be required for cell survival, and therefore, may not represent the response of normal cells in vivo [31, 46]. Previous studies have reported significant differences between cell lines and primary cells [47]. BMDM

were used in this study to confirm and compare the results from the macrophage cell line and to observe the effects of ND on these cells during their differentiation.

Microscopic images showed that these cells internalized ND into their cytoplasm without any significant effect on cell shape. However, ND-treated cells appeared larger in these images owing to their darker color compared to the transparent control cells. FACS results showed that these cells decreased in size in response to ND (26-32% reduction in size). Other studies showed that macrophages and other cell types increased in size in response to ND treatment [48, 49]. In these studies, the size of the ND was 10 times smaller than our ND (< 10 nm), which tends to have more harmful effects on cells [17, 50]. FACS results also showed an increase in cellular granularity, which has also been reported previously [49]. The internalized ND remained in the cytoplasm of these cells, which has also been reported in previous studies but for other cell types [12, 13].

The bright fluorescence of the ND was efficiently captured using fluorescence microscopy and FACS. The fluorescence intensity increased with increasing ND concentrations or treatment intervals. The intrinsic fluorescence of the ND arises from the presence of negatively charged nitrogen vacancy centers [51]. This stable fluorescence makes the ND suitable for imaging and tracking applications [52]. The uptake of these particles was shown to be dependent on the concentration and treatment intervals, as well as the size of the particles and cell types [13, 53]. The uptake mechanism of nanoparticles depends on their specific characteristics and cell type [54]. We used different endocytic pathway inhibitors to study the uptake mechanism of ND in these cells, which showed that the uptake was reduced by approximately 40% when using the inhibitor of actin-dependent pathways and by approximately 20% when using the inhibitor of clathrin-dependent pathways. Other cell types have been reported to internalize ND via a clathrin-dependent pathway [53]. Professional phagocytes, such as macrophages, can endocytose particles of varying sizes through phagocytosis, which is actin-dependent; however, this does not preclude endocytosis through other pathways. Huang et al. showed that ND internalization in RAW264.7 macrophages was reduced by 23% using the same clathrin pathway inhibitor but at lower concentrations [55]. However, they did not report any effects of an actin pathway inhibitor.

The fact that these particles can be clearly detected inside the cells is beneficial, especially for tracking and imaging applications. However, this feature can be problematic because it can interfere with the colorimetric and fluorometric assays. We showed that ND can absorb light at different wavelengths, and they also interfere with fluorescence signals at different wavelengths; therefore, attention should be paid when assessing the effects of these particles on cells, for example, for viability assays. The interference of nanoparticles with toxicity assays has been previously reported for different particles [56, 57]. We used the MTS assay because the detection of cell metabolic activity does not require cell lysis to release the formazan produced. Our results showed no significant reduction in cell viability after exposure to ND at different concentrations and time points. Similarly, previous studies showed no significant effects of ND on different cell types [7, 55]. These studies used the MTT assay, which requires measurement of the absorbance at 570 and 690 nm, which we have observed to have ND interference. A more recent study showed a reduction of approximately 14% in cell viability in response to ND-COOH, which was functionalized from smaller (4-5 nm) pristine ND [58].

The expression of inflammatory cytokines and chemokines was studied at the mRNA and protein levels, and the results showed no significant difference between ND-treated and untreated cells. Although we did not observe statistically significant changes in gene expression, the results clearly showed differences in responses between the two cell types. The proinflammatory cytokines and chemokines interleukin (IL)1 β , CCL2, and CXCL2 were significantly upregulated in three out of the four replicated experiments using J774A.1. However, only CXCL2 was upregulated in BMDM. Previous studies have reported dif-

ferent results regarding the regulation of the expression of various pro- and anti-inflammatory cytokines. Huang et al. showed that small (2-8 nm) ND had no effect on the expression of IL6, TNF α , and iNOS in a murine macrophage cell line [55]. Another study also showed downregulation in the expression of IL1 β , TNF α , CXCL2, CCL2, PDGF, and VEGF in the same cell type (RAW 264.7) in response to different sizes of ND [17]. Other studies also reported no significant production of pro-inflammatory cytokines in these cells [55, 59]. Expression of TNF α , but not IFN γ , increases in response of human monocytes to ND without upregulating the expression of activation markers [60]. In contrast, carboxylated ND induces inflammatory cytokines in monocytes [58]. However, this study used a different cell type and much smaller particles than those used in the ND. Another recent study also showed significant expression of inflammatory cytokines in a monocyte cell line [61]. The variations in the changes in gene expression can be explained by the type of cells and particles being studied.

The ability of different nanoparticles to modulate or inhibit the immune functions of macrophages has been reported; therefore, we aimed to study the effects of ND on two main macrophage functions. Cells were pre-treated with ND before exposure to the conventional macrophage activator LPS. The responses of the two cell types were then assessed using RT-qPCR. The results showed that both ND-treated and untreated cells were able to respond normally to LPS. To our knowledge, the effect of ND on the ability of macrophages to respond to LPS has not yet been investigated. The ability of RAW 264.7 cells has been shown to be attenuated in response to CpG (TLR9 ligand) treatment with gold nanoparticles [62]. Further studies are needed to investigate the effects of ND on the response of macrophages to other immunogens and ND concentrations.

The endocytic activity of macrophages after treatment with ND has also been studied, and the results showed a significant decrease in the ability of these cells to internalize dextran particles. The endocytic activity of macrophages after exposure to ND has not been studied, but other nanoparticles have been shown to reduce this activity [63-65]. In these studies, the nanoparticles did not induce a significant reduction in cell death or inflammatory response; rather, they showed interference in macrophage functions, such as response to LPS and phagocytic activity. These results show that different nanoparticles might be used to manipulate the functions or responses of immune cells for different therapeutic purposes.

The primary macrophages used in this study were prepared from mouse bone marrow under M-CSF. We studied the effects of ND on differentiating cells and found that cell morphology did not change in response to ND treatment. In addition, the percentage of cells expressing the macrophage surface markers (CD11b and F480) did not change. However, the number of surface markers expressed on these cells was significantly reduced, which may indicate an effect on the macrophage function. These markers are required for various macrophage functions including cell adhesion, spreading, and migration [66]. Previous studies have shown significant changes in the ability of macrophages to

phagocytose opsonized and non-opsonized beads after exposure to different nanoparticles [67]. An in vivo study in chicken embryos showed that ND may interfere with cell differentiation by downregulating growth factors [68].

Several previous studies have investigated the effects of different types of ND on cell viability, but few have investigated their effects on macrophage function. To the best of our knowledge, the effects of ND on BMDM during and after differentiation have not yet been investigated. Further studies are needed to investigate the effects of ND on macrophage function, and the mechanisms by which these particles interfere with macrophage function. The responses of different cell types may vary significantly; therefore, it is essential to study the interactions of different nanoparticles in different systems before concluding their toxic/nontoxic effects. In addition, it is important to note the ability of these particles to interfere with both the absorbance and fluorescence signals, which may lead to false results in toxicity studies.

Conclusion

Our findings suggest that ND is not cytotoxic to the macrophage cell line and the primary cells at the tested concentrations, but it can interfere with macrophage functions and differentiation and may interfere with different colorimetric and fluorometric assay results through the production of a signal at different wavelengths.

List of abbreviations

- µg Microgram
- ANOVA Analysis of variance
- BMDM Bone marrow derived macrophages
- CCL C-C motif ligand
- cDNA Complimentary DNA
- CPZ Chlorpromazine hydrochloride
- ct Threshold cycle
- CXCL C-X-C motif ligand
- CYTO Cytochalasin D
- DMSO Dimethyl sulfoxide
- DNA Deoxyribonucleic acid
- EIPA 5-(N-Ethyl-N-isopropyl) amiloride
- FACS Fluorescence-activated cell sorting
- FBS Fetal bovine serum
- GAPDH Glyceraldehyde 3-phosphate dehydrogenase
- IACUC Institutional animal care and use committee
- IFN Interferon
- IL Interleukin
- iNOS Inducible nitric oxide synthase
- LPS Lipopolysaccharide
- MBC Methyl-beta-cyclodextrin
- M-CSF Macrophage-colony stimulating factor
- MFI Mean fluorescence intensity
- ND Nanodiamonds
- ng Nanogram
- nm Nanometer
- NV Nitrogen vacancy
- NYST Nystatin
- OD Optical density
- PBS Phosphate buffer saline
- PDGF Platelet-derived growth factor
- PHYN Phenylarsine oxide
- RNA Ribonucleic acid
- ROS Reactive oxygen species
- RT-qPCR Real time-quantitative polymerase chain reaction
- SEM Standard error mean
- SSC Side scatter
- TNF Tumor necrosis factor
- VEGF Vascular-endothelial growth factor

References

1. McNamara, K., & Tofail, S. A. (2017). Nanoparticles in biomedical applications. *Advances in Physics: X*, 2(1), 54-88.
2. Khan, I., Saeed, K., & Khan, I. (2019). Nanoparticles: Properties, applications and toxicities. *Arabian journal of chemistry*, 12(7), 908-931.
3. Fisher, C., Rider, A. E., Han, Z. J., Kumar, S., Levchenko, I., & Ostrikov, K. (2012). Applications and nanotoxicity of carbon nanotubes and graphene in biomedicine. *Journal of Nanomaterials*, 2012, 1-19.
4. Khabashesku, V. N., Margrave, J. L., & Barrera, E. V. (2005). Functionalized carbon nanotubes and nanodiamonds for engineering and biomedical applications. *Diamond and Related Materials*, 14(3-7), 859-866.
5. Patel, K. D., Singh, R. K., & Kim, H. W. (2019). Carbon-based nanomaterials as an emerging platform for therapeutics. *Materials Horizons*, 6(3), 434-469.
6. Stacey, M., Osgood, C., Kalluri, B. S., Cao, W., Elsayed-Ali, H., & Abdel-Fattah, T. (2011). Nanosecond pulse electrical fields used in conjunction with multi-wall carbon nanotubes as a potential tumor treatment. *Biomedical Materials*, 6(1), 011002.
7. Schrand, A. M., Huang, H., Carlson, C., Schlager, J. J., Ōsawa, E., Hussain, S. M., & Dai, L. (2007). Are diamond nanoparticles cytotoxic?. *The journal of physical chemistry B*, 111(1), 2-7.
8. Kaur, R., & Badea, I. (2013). Nanodiamonds as novel nanomaterials for biomedical applications: drug delivery and imaging systems. *International journal of nanomedicine*, 203-220.
9. Perevedentseva, E., Lin, Y. C., Jani, M., & Cheng, C. L. (2013). Biomedical applications of nanodiamonds in imaging and therapy. *Nanomedicine*, 8(12), 2041-2060.
10. Lim, D. G., Kim, K. H., Kang, E., Lim, S. H., Ricci, J., Sung, S. K., ... & Jeong, S. H. (2016). Comprehensive evaluation of carboxylated nanodiamond as a topical drug delivery system. *International journal of nanomedicine*, 11, 2381.
11. Vijayanthimala, V., Lee, D. K., Kim, S. V., Yen, A., Tsai, N., Ho, D., ... & Shenderova, O. (2015). Nanodiamond-mediated drug delivery and imaging: challenges and opportunities. *Expert opinion on drug delivery*, 12(5), 735-749.
12. Yu, S. J., Kang, M. W., Chang, H. C., Chen, K. M., & Yu, Y. C. (2005). Bright fluorescent nanodiamonds: no photobleaching and low cytotoxicity. *Journal of the American Chemical Society*, 127(50), 17604-17605.
13. Liu, K. K., Cheng, C. L., Chang, C. C., & Chao, J. I. (2007). Biocompatible and detectable carboxylated nanodiamond

- on human cell. *Nanotechnology*, 18(32), 325102.
14. Schrand, A. M., Dai, L., Schlager, J. J., Hussain, S. M., & Osawa, E. (2007). Differential biocompatibility of carbon nanotubes and nanodiamonds. *Diamond and Related Materials*, 16(12), 2118-2123.
 15. Mansoorianfar, M., Shokrgozar, M. A., Mehrjoo, M., Tamjid, E., & Simchi, A. (2013). Nanodiamonds for surface engineering of orthopedic implants: enhanced biocompatibility in human osteosarcoma cell culture. *Diamond and related materials*, 40, 107-114.
 16. Dworak, N., Wnuk, M., Zebrowski, J., Bartosz, G., & Lewinska, A. (2014). Genotoxic and mutagenic activity of diamond nanoparticles in human peripheral lymphocytes in vitro. *Carbon*, 68, 763-776.
 17. Thomas, V., Halloran, B. A., Ambalavanan, N., Catledge, S. A., & Vohra, Y. K. (2012). In vitro studies on the effect of particle size on macrophage responses to nanodiamond wear debris. *Acta biomaterialia*, 8(5), 1939-1947.
 18. Lin, Y. C., Wu, K. T., Lin, Z. R., Perevedentseva, E., Karmenyan, A., Lin, M. D., & Cheng, C. L. (2016). Nanodiamond for biolabelling and toxicity evaluation in the zebrafish embryo in vivo. *Journal of biophotonics*, 9(8), 827-836.
 19. Karpeta-Kaczmarek, J., Kędziorski, A., Augustyniak-Jabłokow, M. A., Dziewięcka, M., & Augustyniak, M. (2018). Chronic toxicity of nanodiamonds can disturb development and reproduction of *Acheta domesticus* L. *Environmental research*, 166, 602-609.
 20. Ray, P., Haideri, N., Haque, I., Mohammed, O., Chakraborty, S., Banerjee, S., ... & Banerjee, S. K. (2021). The impact of nanoparticles on the immune system: a gray zone of nanomedicine. *Journal of Immunological Sciences*, 5(1).
 21. Wang, X., Reece, S. P., & Brown, J. M. (2013). Immunotoxicological impact of engineered nanomaterial exposure: mechanisms of immune cell modulation. *Toxicology mechanisms and methods*, 23(3), 168-177.
 22. Yazdi, A. S., Guarda, G., Riteau, N., Drexler, S. K., Tardivel, A., Couillin, I., & Tschopp, J. (2010). Nanoparticles activate the NLR pyrin domain containing 3 (Nlrp3) inflammasome and cause pulmonary inflammation through release of IL-1 α and IL-1 β . *Proceedings of the National Academy of Sciences*, 107(45), 19449-19454.
 23. Yang, E. J., Kim, S., Kim, J. S., & Choi, I. H. (2012). Inflammasome formation and IL-1 β release by human blood monocytes in response to silver nanoparticles. *Biomaterials*, 33(28), 6858-6867.
 24. Schanen, B. C., Karakoti, A. S., Seal, S., Drake III, D. R., Warren, W. L., & Self, W. T. (2009). Exposure to titanium dioxide nanomaterials provokes inflammation of an in vitro human immune construct. *ACS nano*, 3(9), 2523-2532.
 25. Salvador-Morales, C., Flahaut, E., Sim, E., Sloan, J., Green, M. L., & Sim, R. B. (2006). Complement activation and protein adsorption by carbon nanotubes. *Molecular immunology*, 43(3), 193-201.
 26. Dutta, D., Sundaram, S. K., Teeguarden, J. G., Riley, B. J., Fifield, L. S., Jacobs, J. M., ... & Weber, T. J. (2007). Adsorbed proteins influence the biological activity and molecular targeting of nanomaterials. *Toxicological Sciences*, 100(1), 303-315.
 27. Mitchell, L. A., Lauer, F. T., Burchiel, S. W., & McDonald, J. D. (2009). Mechanisms for how inhaled multiwalled carbon nanotubes suppress systemic immune function in mice. *Nature nanotechnology*, 4(7), 451-456.
 28. Brown, D. M., Kinloch, I. A., Bangert, U., Windle, A. H., Walter, D. M., Walker, G. S., ... & Stone, V. I. C. K. I. (2007). An in vitro study of the potential of carbon nanotubes and nanofibres to induce inflammatory mediators and frustrated phagocytosis. *Carbon*, 45(9), 1743-1756.
 29. Murphy, F. A., Schinwald, A., Poland, C. A., & Donaldson, K. (2012). The mechanism of pleural inflammation by long carbon nanotubes: interaction of long fibres with macrophages stimulates them to amplify pro-inflammatory responses in mesothelial cells. *Particle and fibre toxicology*, 9(1), 1-15.
 30. Weischenfeldt, J., & Porse, B. (2008). Bone marrow-derived macrophages (BMM): isolation and applications. *Cold Spring Harbor Protocols*, 2008(12), pdb-prot5080.
 31. Marim, F. M., Silveira, T. N., Lima Jr, D. S., & Zamboni, D. S. (2010). A method for generation of bone marrow-derived macrophages from cryopreserved mouse bone marrow cells. *PloS one*, 5(12), e15263.
 32. Wang, L. H., Rothberg, K. G., & Anderson, R. G. (1993). Mis-assembly of clathrin lattices on endosomes reveals a regulatory switch for coated pit formation. *The Journal of cell biology*, 123(5), 1107-1117.
 33. Shamsul, H. M., Hasebe, A., Iyori, M., Ohtani, M., Kiura, K., Zhang, D., ... & Shibata, K. I. (2010). The Toll-like receptor 2 (TLR2) ligand FSL-1 is internalized via the clathrin-dependent endocytic pathway triggered by CD14 and CD36 but not by TLR2. *Immunology*, 130(2), 262-272.
 34. Gibson, A. E., Noel, R. J., Herlihy, J. T., & Ward, W. F. (1989). Phenylarsine oxide inhibition of endocytosis: effects on asialofetuin internalization. *American Journal of Physiology-Cell Physiology*, 257(2), C182-C184.
 35. Cai, Y., Postnikova, E. N., Bernbaum, J. G., Yú, S., Mazur, S., Deiuliis, N. M., ... & Kuhn, J. H. (2015). Simian hemorrhagic fever virus cell entry is dependent on CD163 and uses a clathrin-mediated endocytosis-like pathway. *Journal of virology*, 89(1), 844-856.
 36. Rodal, S. K., Skretting, G., Garred, Ø., Vilhardt, F., Van Deurs, B., & Sandvig, K. (1999). Extraction of cholesterol with methyl- β -cyclodextrin perturbs formation of clathrin-coated endocytic vesicles. *Molecular biology of the cell*, 10(4), 961-974.
 37. Li, Y. L., Van Cuong, N., & Hsieh, M. F. (2014). Endocytosis pathways of the folate tethered star-shaped PEG-PCL micelles in cancer cell lines. *Polymers*, 6(3), 634-650.
 38. Payne, C. K., Jones, S. A., Chen, C., & Zhuang, X. (2007). Internalization and trafficking of cell surface proteoglycans and proteoglycan-binding ligands. *Traffic*, 8(4), 389-401.
 39. West, M. A., Bretscher, M. S., & Watts, C. (1989). Distinct endocytotic pathways in epidermal growth factor-stimulated human carcinoma A431 cells. *The Journal of cell biology*, 109(6), 2731-2739.
 40. Gerondopoulos, A., Jackson, T., Monaghan, P., Doyle, N., & Roberts, L. O. (2010). Murine norovirus-1 cell entry is mediated through a non-clathrin-, non-caveolae-, dynamin-and

- cholesterol-dependent pathway. *Journal of General Virology*, 91(6), 1428-1438.
41. Sampath, P., & Pollard, T. D. (1991). Effects of cytochalasin, phalloidin and pH on the elongation of actin filaments. *Biochemistry*, 30(7), 1973-1980.
 42. Osterholzer, J. J., Chen, G. H., Olszewski, M. A., Zhang, Y. M., Curtis, J. L., Huffnagle, G. B., & Toews, G. B. (2011). Chemokine receptor 2-mediated accumulation of fungicidal exudate macrophages in mice that clear cryptococcal lung infection. *The American journal of pathology*, 178(1), 198-211.
 43. Martinon, F., Chen, X., Lee, A. H., & Glimcher, L. H. (2010). Toll-like receptor activation of XBP1 regulates innate immune responses in macrophages. *Nature immunology*, 11(5), 411.
 44. Santoro, A., Ferrante, M. C., Di Guida, F., Pirozzi, C., Lama, A., Simeoli, R., ... & Meli, R. (2015). Polychlorinated biphenyls (PCB 101, 153, and 180) impair murine macrophage responsiveness to lipopolysaccharide: involvement of NF- κ B pathway. *Toxicological Sciences*, 147(1), 255-269.
 45. Liu, T., Shi, Y., Du, J., Ge, X., Teng, X., Liu, L., ... & Zhao, Q. (2016). Vitamin D treatment attenuates 2, 4, 6-trinitrobenzene sulphonic acid (TNBS)-induced colitis but not oxazolone-induced colitis. *Scientific reports*, 6(1), 32889.
 46. Kaur, G., & Dufour, J. M. (2012). Cell lines: Valuable tools or useless artifacts. *Spermatogenesis*, 2(1), 1-5.
 47. Chamberlain, L. M., Godek, M. L., Gonzalez-Juarrero, M., & Grainger, D. W. (2009). Phenotypic non-equivalence of murine (monocyte-) macrophage cells in biomaterial and inflammatory models. *Journal of Biomedical Materials Research Part A: An Official Journal of The Society for Biomaterials, The Japanese Society for Biomaterials, and The Australian Society for Biomaterials and the Korean Society for Biomaterials*, 88(4), 858-871.
 48. Mytych, J., Lewinska, A., Bielak-Zmijewska, A., Grabowska, W., Zebrowski, J., & Wnuk, M. (2014). Nanodiamond-mediated impairment of nucleolar activity is accompanied by oxidative stress and DNMT2 upregulation in human cervical carcinoma cells. *Chemico-biological interactions*, 220, 51-63.
 49. Mytych, J., Lewinska, A., Zebrowski, J., & Wnuk, M. (2015). Nanodiamond-induced increase in ROS and RNS levels activates NF- κ B and augments thiol pools in human hepatocytes. *Diamond and Related Materials*, 55, 95-101.
 50. Keremidarska, M., Ganeva, A., Mitev, D., Hikov, T., Presker, R., Pramatarova, L., & Krasteva, N. (2014). Comparative study of cytotoxicity of detonation nanodiamond particles with an osteosarcoma cell line and primary mesenchymal stem cells. *Biotechnology & Biotechnological Equipment*, 28(4), 733-739.
 51. Davies, G., Lawson, S. C., Collins, A. T., Mainwood, A., & Sharp, S. J. (1992). Vacancy-related centers in diamond. *Physical Review B*, 46(20), 13157.
 52. Shenderova, O. A., & McGuire, G. E. (2015). Science and engineering of nanodiamond particle surfaces for biological applications. *Biointerphases*, 10(3), 030802.
 53. Perevedentseva, E., Hong, S. F., Huang, K. J., Chiang, I. T., Lee, C. Y., Tseng, Y. T., & Cheng, C. L. (2013). Nanodiamond internalization in cells and the cell uptake mechanism. *Journal of nanoparticle research*, 15, 1-12.
 54. Iversen, T. G., Skotland, T., & Sandvig, K. (2011). Endocytosis and intracellular transport of nanoparticles: Present knowledge and need for future studies. *Nano today*, 6(2), 176-185.
 55. Huang, K. J., Lee, C. Y., Lin, Y. C., Lin, C. Y., Perevedentseva, E., Hung, S. F., & Cheng, C. L. (2017). Phagocytosis and immune response studies of Macrophage-Nanodiamond Interactions in vitro and in vivo. *Journal of biophotonics*, 10(10), 1315-1326.
 56. Wörle-Knirsch, J. M., Pulskamp, K., & Krug, H. F. (2006). Oops they did it again! Carbon nanotubes hoax scientists in viability assays. *Nano letters*, 6(6), 1261-1268.
 57. Kroll, A., Pillukat, M. H., Hahn, D., & Schneckeburger, J. (2012). Interference of engineered nanoparticles with in vitro toxicity assays. *Archives of toxicology*, 86, 1123-1136.
 58. Fusco, L., Avitabile, E., Armuzza, V., Orecchioni, M., Istif, A., Bedognetti, D., ... & Delogu, L. G. (2020). Impact of the surface functionalization on nanodiamond biocompatibility: A comprehensive view on human blood immune cells. *Carbon*, 160, 390-404.
 59. Huang, H., Pierstorff, E., Osawa, E., & Ho, D. (2008). Protein-mediated assembly of nanodiamond hydrogels into a biocompatible and biofunctional multilayer nanofilm. *ACS nano*, 2(2), 203-212.
 60. Suarez-Kelly, L. P., Campbell, A. R., Rampersaud, I. V., Bumb, A., Wang, M. S., Butchar, J. P., ... & Carson III, W. E. (2017). Fluorescent nanodiamonds engage innate immune effector cells: A potential vehicle for targeted anti-tumor immunotherapy. *Nanomedicine: Nanotechnology, Biology and Medicine*, 13(3), 909-920.
 61. Knotigova, P. T., Mašek, J., Hubatka, F., Kotouček, J., Kulich, P., Simeckova, P., ... & Turánek, J. (2019). Application of advanced microscopic methods to study the interaction of carboxylated fluorescent nanodiamonds with membrane structures in THP-1 cells: Activation of inflammasome NLRP3 as the result of lysosome destabilization. *Molecular Pharmaceutics*, 16(8), 3441-3451.
 62. Tsai, C. Y., Lu, S. L., Hu, C. W., Yeh, C. S., Lee, G. B., & Lei, H. Y. (2012). Size-dependent attenuation of TLR9 signaling by gold nanoparticles in macrophages. *The Journal of immunology*, 188(1), 68-76.
 63. Kodali, V., Littke, M. H., Tilton, S. C., Teeguarden, J. G., Shi, L., Frevert, C. W., ... & Thrall, B. D. (2013). Dysregulation of macrophage activation profiles by engineered nanoparticles. *ACS nano*, 7(8), 6997-7010.
 64. Fuchs, A. K., Syrovets, T., Haas, K. A., Loos, C., Musyanovych, A., Mailänder, V., ... & Simmet, T. (2016). Carboxyl- and amino-functionalized polystyrene nanoparticles differentially affect the polarization profile of M1 and M2 macrophage subsets. *Biomaterials*, 85, 78-87.
 65. Huang, C., Sun, M., Yang, Y., Wang, F., Ma, X., Li, J., ... & Wang, H. (2017). Titanium dioxide nanoparticles prime a specific activation state of macrophages. *Nanotoxicology*, 11(6), 737-750.
 66. Solovjov, D. A., Pluskota, E., & Plow, E. F. (2005). Distinct

-
- roles for the α and β subunits in the functions of integrin α M β 2. *Journal of biological chemistry*, 280(2), 1336-1345.
67. DeLoid, G., Casella, B., Pirela, S., Filoramo, R., Pyrgiotakis, G., Demokritou, P., & Kobzik, L. (2016). Effects of engineered nanomaterial exposure on macrophage innate immune function. *NanoImpact*, 2, 70-81.
68. Wierzbicki, M., Sawosz, E., Grodzik, M., Hotowy, A., Prasek, M., Jaworski, S., ... & Chwalibog, A. (2013). Carbon nanoparticles downregulate expression of basic fibroblast growth factor in the heart during embryogenesis. *International journal of nanomedicine*, 3427-3435

Copyright: ©2023 Christopher Osgood, et al. This is an open-access article distributed under the terms of the Creative Commons Attribution License, which permits unrestricted use, distribution, and reproduction in any medium, provided the original author and source are credited.